Metabolite Profiling of Whole Murine Embryos Reveals Metabolic Perturbations Associated with Maternal Valproate-Induced Neural Tube Closure Defects

Darya Akimova[¶,⌘], **Bogdan J. Wlodarczyk**[∥], **Ying Lin**[∥], **M. Elizabeth Ross**[§], **Richard H. Finnell**[∥], **Qiuying Chen**[¶], and **Steven S. Gross**[¶]

[¶]Department of Pharmacology, Weill Cornell Medical College, New York, NY 10021

[§]Feil Family Brain and Mind Research Institute, Weill Cornell Medical College, New York, NY 10021

[⌘]Program in Pharmacology, Weill Cornell Medical College, New York, NY 10021

[∥]Department of Nutritional Sciences, Dell Pediatric Research Institute, The University of Texas at Austin, Austin TX 78723

Abstract

Background—Valproic Acid (VPA) is prescribed therapeutically for multiple conditions, including epilepsy. When taken during pregnancy, VPA is teratogenic, increasing the risk of several birth and developmental defects including neural tube defects (NTDs). The mechanism by which VPA causes NTDs remains controversial and how VPA interacts with folic acid, a vitamin commonly recommended for the prevention of NTDs, remains uncertain. We sought to address both questions by applying untargeted metabolite profiling analysis to neural tube closure stage mouse embryos.

Methods—Pregnant SWV dams on either a 2ppm or 10ppm folic acid (FA) supplemented diet were injected with a single dose of VPA on gestational day E8.5. On day E9.5, the mouse embryos were collected and evaluated for neural tube closure status. LC/MS metabolomics analysis was performed to compare metabolite profiles of NTD-affected VPA-exposed whole mouse embryos to profiles from embryos that underwent normal neural tube closure from control dams.

Results—NTDs were observed in all embryos from VPA-treated dams and penetrance was not diminished by dietary folic acid supplementation. The most profound metabolic perturbations were found in the 10ppm FA VPA-exposed mouse embryos, compared to the other three treatment groups. Affected metabolites included amino acids, nucleobases and related phosphorylated nucleotides, lipids, and carnitines.

Conclusions—Maternal VPA treatment markedly perturbed purine and pyrimidine metabolism in E9.5 embryos. In combination with a high folic acid diet, VPA treatment resulted in gross metabolic changes, likely caused by a multiplicity of mechanisms, including an apparent disruption of mitochondrial beta-oxidation.

Address correspondence to: Dr. Steven Gross, 1300 York Ave, New York, NY 10021, Fax: 212-746-8835, ssgross@med.cornell.edu.

Introduction

Neural tube closure (NTC) involves complex, coordinated cellular programs such as gene transcription switches, cell migration, differentiation, proliferation, and growth (Sadler, 2005; Wilde et al., 2014). Neural tube defects (NTDs) are a family of congenital malformations that are the likely result from a failure in one or more of these processes that impede proper neural fold fusion, and lead to detrimental or even lethal consequences for the developing embryo (Wallingford et al., 2013; Greene and Copp, 2014). The complex synchronization of multiple morphogenetic processes required for proper NTC, as well as the relatively narrow developmental time frame allowed for completion, may explain why NTDs are one of the most common birth defects. In addition, given their complex etiology, NTDs remain one of the least well-understood birth defects. Multiple environmental factors and more than 400 genetic mutations have been implicated as NTD risk factors in the mouse, making NTD-prevention a significant challenge for society.

Valproic acid (VPA) is a branched chain carboxylic acid that has been prescribed for over four decades in the treatment of epilepsy, mood disorders, and migraine, and has been evaluated in clinical trials for therapy of cancer and HIV. In epilepsy, its first approved indication, VPA has been shown to be effective against several types of seizures, including tonic-clonic, absence, and myoclonic (Buourgeois, 2002; Marson and Sills, 2015). VPA also has an important niche in migraine and mood disorder treatment, especially in patients that suffer from both epilepsy and bipolar disorder, particularly in cases where lithium has proven to be ineffective (Silberstein, 2002; Swann, 2002; Marson and Sills, 2015). The adverse effects associated with VPA therapy are well documented after its longtime use, with hepatotoxicity and teratogenicity being some of the more severe undesired outcomes. Children of women who are treated with VPA during pregnancy are at a higher risk of cleft palate, cardiovascular malformations, craniosynostosis, developmental delay and NTDs, particularly spina bifida (Jentink et al., 2010b; Meador et al., 2006). The three predominant proposed mechanisms for VPA-induced teratogenesis are generation of oxidative stress, histone deacetylase (HDAC) inhibition, and perturbation of folate metabolism (Göttlicher et al., 2001; Ornoy, 2009; Tung and Winn, 2011; Lloyd, 2013; Fathe et al., 2014).

Folic acid supplementation is recommended for all women during pregnancy. It has been shown to prevent NTDs in large scale epidemiological studies and in certain animal models, but the mechanism by which it does so remains controversial (Copp et al., 2013). Women who have had an NTD-affected pregnancy or who are on anti-convulsant drug therapy are recommended to consume up to 5 mg per day of folic acid. Whether maternal folate supplementation is sufficient to prevent VPA-induced teratogenicity is a matter of considerable clinical interest and controversy, with conflicting reports from epidemiological and laboratory studies (Elmazar et al., 1992; Hansen et al., 1995; Ornoy, 2009; Jentink et al.,

2010a). Thus, demonstrating the impact of exogenous folates in VPA treated women is of great therapeutic importance. A powerful approach to broadly survey metabolic perturbations that may occur in response to drugs and diet is untargeted metabolic profiling.

Metabolite profiling can utilize the power of liquid chromatography coupled to mass spectrometry (LC/MS) to identify and quantify the relative levels of diverse metabolites in complex biological samples. Knowledge of metabolite profiles can provide a direct readout of the embryo's metabolic status and potentially reveal the underlying molecular bases for drug-induced birth defects. As the final common output of genes, transcripts, and protein activities, the metabolome offers the most proximal molecular readout for birth defect causation. We previously showed that this approach can be effectively applied to assess the metabolic actions of diverse factors known to contribute to NTDs in environmental and genetic mouse models (Hansler et al., 2014).

Here we demonstrate the application of LC/MS-based metabolomic analysis to a comparison of NTD-affected vs. control E9.5 whole mouse embryos from dams maintained on either a relatively high (10ppm) or low (2ppm) folic acid diet and administered a single dose of VPA (or solvent control) on day E8.5 of pregnancy. The results demonstrate that VPA treatment significantly and predominantly impacts purine and pyrimidine metabolism. Interestingly, increased folic acid supplementation was not only ineffective in preventing the development of NTDs, but mouse embryos from VPA-treated dams receiving the high folic acid diet presented with more severe metabolic aberrations than did embryos of VPA-treated dams on a low folic acid diet. These more severe metabolic aberrations included altered levels of lipids, acyl-carnitines, amino acids, and one-carbon cycle intermediates, pointing to an interaction between a high folic acid diet and VPA treatment. The finding that high folic acid supplementation can worsen *in utero* metabolic defects in VPA-exposed embryos and the relatively unexplored role of defective mitochondrial beta-oxidation as a driver of NTDs both offer potentially important avenues for future investigation.

Materials and Methods

Mouse Breeding and Embryo Harvest

All procedures involving animals were carried out in accordance with the guidelines established by the NIH and IACUC of Weill Cornell Medical College and the University of Texas at Austin. Mice were housed in the UT Austin animal facility on a 12 hr light-dark cycle and placed on a diet of lab chow containing either 2ppm or 10ppm folic acid (FA), constituting relatively low- and high-FA diets. Mating pairs of SWV strain mice were set in the late afternoon by introducing males to females. The following morning (putative embryonic day E0.5), males and females were separated and potential pregnancies were determined by the presence of a vaginal plug. Female mice were weighed immediately, and then again at day 7 to assess weight gain, indicative of continued pregnancy. If a plug was apparent following mating, dams were administered a single treatment with 2.7 mmol/kg sodium valproate (VPA) on day E8.5. Dams that gained over 2.5g of weight by E9.5 were considered pregnant and euthanized at E9.5. The uterus was removed and placed into ice-cold phosphate-buffered saline (PBS) for dissection. Individual implantations were dissected free from the decidua, visually inspected, and scored for somite staging as well as the

presence or absence of NTDs. Dissection, somite scoring, and NTD scoring were conducted with the aid of a Leica dissection microscope and images were saved to hard disk via camera. Embryos were then washed briefly in dH_2O to remove excess PBS and snap frozen on dry ice. Each treatment group included embryos collected from 2 dams and, therefore, 8 dams in total were included in this study.

Metabolite Extraction from Whole Mouse Embryos

Embryonic metabolism was quenched by adding 400μL cold 80:20 Methanol (Optima LC/MS Grade, Fisher Chemical):ddH2O to each mouse embryo on ice. Steel beads (Cat No. 69989, Qiagen) and a TissueLyser II (Qiagen) were used to lyse the embryos and extract metabolites. The homogenized samples were centrifuged at 14,000 rpm at 4°C for 10 min. The supernatant (i.e., the methanolic metabolite extract), was collected and the pellet was homogenized twice more in a fresh volume of 80:20 methanol:ddH_2O, followed by centrifugation. Supernatants from all successive homogenization and centrifugation steps was pooled for a total volume of 1.2 ml of metabolite extract, corresponding to each individual embryo. The extracts were dried using a vacuum centrifuge (Eppendorf) and the resulting metabolite films were stored at −80°C until LC/MS analysis. Mouse embryo tissue pellets were retained after centrifugation, dried and retained for protein quantification, as described below.

Protein Quantification and Metabolite Extract Normalization

Residual tissue pellets, collected from each embryo after metabolite extraction, were resuspended in 100 μL of 0.2 M NaOH. Pellets were vortexed and heated for 20 min at 95°C and then centrifuged at 7,500 rpm for 12 min. Protein content of the resuspended pellets was quantified using the DC protein assay (Bio-Rad) and bovine serum albumin in 0.2M NaOH as a reference standard. The calculated total protein was used as a normalization value to account for differences in embryo size when metabolite films were resuspended for analysis by LC/MS-based metabolite profiling.

Sample Preparation for Metabolomic Analysis

Based on the protein quantification results, metabolite films from each embryo were resuspended in a volume of 70:30 Acetonitrile (Optima LC/MS Grade, Fisher Chemical):ddH_2O containing 0.2% acetic acid, to what would have been a protein concentration of 2 μg/μl. The reconstituted samples were vortexed and placed at −20°C for 1 hour with occasional vortexing to redissolve metabolites. Samples were then centrifuged at 14,000 rpm at 4°C for 10 min. Supernatants were transferred to 250 μl conical polypropylene HPLC vials, capped, and placed into the LC autosampler at 4°C for analysis by LC/MS.

LC/MS Data Acquisition

Metabolomics data were acquired for each mouse embryo metabolite extract in an untargeted manner, as previously detailed (Hansler et al., 2014). Briefly, each sample was injected onto a 150 mm × 2.1 mm Diamond Hydride HPLC Column (Microsolve) and compounds were separated using aqueous normal phase gradient chromatography

comprising mobile phase A: isopropyl alcohol + acetic acid + EDTA + H_2O and mobile phase B: acetonitrile + ammonium acetate + EDTA. LC flow was directed into an Agilent model 6230 time-of-flight (TOF) mass spectrometer (MS) equipped with a dual electrospray ionization source (ESI). MS data were collected for all samples in both negative ion-monitoring mode and positive ion-monitoring mode within the mass to charge window of 50.0 to 1000.0 m/z.

Data Analysis

Acquired MS-TOF data files were processed using Agilent Profinder Software (Version B. 06.00). An in-house aqueous normal phase chromatography database, comprised of 801 compounds annotated by structural identity, accurate mass, and chromatographic retention time, was used to quantify the relative abundances of metabolites, based on hydrogen loss as the charge carrier in negative ion-monitoring mode, and proton gain as the charge carrier in positive ion-monitoring mode, employing a symmetrical *m/z* window of +/− 0.02 Da. A mass window of 20 ppm was considered acceptable for compound identification based on mass and retention time information. MS spectra in centroid mode were analyzed to increase confidence for inferred compound identifications. Abundance information for identified compounds was exported in csv file format and imported into *R* for statistical analysis.

Statistical Analysis

R (Ver 3.2.2) in conjunction with the *RStudio* (Ver 0.99.441) was used for all data analysis procedures. Metabolite measurements were imported into *R* and scaled by subtracting the compound abundance mean across all four groups and dividing by the compound standard deviation across all groups. Sample groups of n = 18 total embryos were analyzed. In cases where the number of embryo samples per group exceeded 18, excess samples were randomly removed for the purpose of a balanced statistical analysis. Two-Way ANOVA was applied to test the effects of maternal VPA treatment, folic acid levels, and the folic acid level-treatment interaction, followed by Benjamini-Hochberg correction to account for multiple tests conducted for each metabolite.

Post-hoc analysis was conducted as follows: for compounds that were found to be significant based on maternal folic acid exposure alone, but not based on the interaction between the two factors, were split based on treatment group (VPA and saline injected) and effects of folic acid level were tested using a t-test, followed by Benjamini-Hochberg multiple hypothesis testing correction for each tested metabolite. For compounds that were found to be significant based on VPA treatment only, but not on the interaction between factors, the groups were divided along folic acid levels (2ppm FA and 10ppm FA) and the effect of treatment was determined by applying a t-test to each group, comparing VPA treatment to saline control, followed by Benjamini-Hochberg multiple hypothesis testing correction. For compounds that were found to be significant based on the VPA treatment-folic acid supplementation interaction, the Tukey HSD test was applied, with Benjamini-Hochberg correction for the number of Tukey HSD tests carried out. For simplicity, only the results of the post hoc tests are considered in the *Results* and *Discussion* sections. Where the text references the result of a t-test, the compound was found to be significantly impacted by either parameter only, but not by their interaction. For compounds that were found to be

significantly impacted by the interaction of the two parameters, Tukey HSD results are presented, along with the statistically significant pairwise comparisons detected by this test.

Principal component analysis was performed using the prcomp function in the standard *R* package. A scree plot was used to determine the number of principal components to be retained for analysis. For data gathered in negative ion-monitoring mode, all principal components after the fourth component were relatively small and decreased at a steady rate, therefore only the first four components were retained because they explained the most meaningful proportion of the observed variance. For positive ion-monitoring mode data, three components were judged to be sufficient to explain the most meaningful proportion of the observed variance. For principal component regression, the data were split into four groups based on treatment and maternal folic acid exposure level, and each principal component that was retained was regressed onto the somite count for each individual embryo. The mixOmics package was used to generate hierarchical cluster plots using the cim function. Clustering was based on the Pearson correlation as the distance metric and the complete clustering method for both columns and rows. The ggplot2 package was used to generate boxplots and to generate PC regression plots.

Results

Data overview

There have been conflicting literature reports regarding whether or not folic acid can effectively prevent VPA-associated teratogenesis in experimental model systems. We observed that a one-time maternal VPA treatment at E8.5 resulted in NTDs in all mouse embryos, regardless of maternal folic acid supplementation levels. While no overt physical phenotype was associated with increased dietary folate, collected mouse embryos were nevertheless separated into four groups: 2ppm FA control, 2ppm FA VPA-exposed, 10ppm FA control, and 10ppm FA VPA-exposed to determine if the two levels of folic acid exposure resulted in distinguishable metabolic phenotypes. Notably, all mouse embryos in the VPA-exposed groups exhibited grossly observable NTDs in the form of exencephaly. In contrast, all mouse embryos from dams that received a control saline injection exhibited normal neural tube closure.

Based on a comparison of LC/MS findings with our aqueous normal phase chromatography in-house database of 801 compounds, 200 compounds with unique mass and retention time were identified across the two MS ion-monitoring modes, with extensive overlap between the two modes. Considering only the major metabolic pathway linked to each metabolite, the identified compounds belonged predominantly to amino acid, lipid, and nucleotide metabolic pathways and had masses ranging from 75.032 to 785.594 Da (Fig 1). It should be noted that VPA and a number of its common predicted metabolites were searched for, but not found in the collected MS data (data not shown). Two-Way ANOVA analysis with Benjamini-Hochberg multiple hypothesis testing correction showed that an astonishing 123 metabolites, out of 146 measured by negative ion mode MS, were statistically different based on the folic acid-treatment interaction, with a large number of these compounds also being significant based on the VPA treatment effect. In addition, 64 out of 121 compounds identified in positive mode were found to be statistically significant based on the treatment

parameter alone. Post hoc analysis for both sets of data revealed that metabolite levels in the 10ppm FA VPA-exposed group were most profoundly perturbed in relation to the other three embryo groups, with most metabolites detected at a relatively diminished abundance.

We considered that the altered metabolic profile of 10ppm FA VPA-exposed mouse embryos may not have been caused by the experimental interventions alone. Indeed, when the embryos were collected, the number of somites was determined for each individual embryo and the number of somites overall for the 10ppm FA VPA-exposed group was observed to be considerably less than that of the other three groups (Fig 2, Table S1). Notably, each of the two litters from 10ppm FA VPA-treated dams offered a range of somite counts within a given litter, with some embryos reaching a "normal" somite count acceptable for E9.5 embryos. It therefore appeared justifiable at the outset of the study to compare groups of embryos of different somite counts and it was assumed that normalization of metabolites to protein content would be sufficient to account for differences in embryo size. However, since the 10ppm FA VPA-exposed embryo group presented the most extreme differences in metabolic profile when compared to the other treatment embryo groups, there was a concern that this outcome was due to the delayed development of the 10ppm FA VPA-exposed embryos, rather than the direct actions of folic acid or VPA treatment.

In a prior study that sought to determine the effect of VPA on the abundance of common metabolites in the urine of epileptic children treated with VPA, it was demonstrated, by applying principal component regression analysis, that a number of compounds correlated in abundance with the age of the child, despite normalization for urinary creatinine levels (Price et al., 2011). The same technique was applied here to determine which metabolites changed in a predictable manner as a function of somite count in the present metabolomics analysis of mouse embryos. Out of the four negative ion-monitoring mode data and the three positive ion-monitoring mode data principal components considered to be sufficient to explain the meaningful proportion of variance in the acquired data, only the linear regression of the second negative mode data principal component (PC2) onto somite count resulted in meaningful R^2 values (Fig 3A-3D, Fig S1A-S1C). Based on this result, a cutoff point of $-2.0 < PC1/PC2 < 2.0$ for any metabolite detected in negative ion-monitoring mode was chosen as the criteria for designating a metabolite as being linked to somite number. A metabolite was judged to be somite-independent if it loaded considerably more onto negative mode PC1 than PC2, or if the data for that metabolite was collected in the positive mode.

Results from a 2ppm Maternal Folic Acid Diet

According to the guidelines of the American Institute of Nutrition for rodent diets, 2ppm folic acid supplementation is considered an acceptable level for maintenance and growth (Reeves, 1997). Therefore, this level of folic acid supplementation can be considered the baseline level and will be discussed first. The only two compounds found statistically significant between the 2ppm FA control and 2ppm FA VPA-exposed groups were adenine and thymine (Table 1). Both metabolites are products of nucleotide breakdown and can either be further degraded and excreted, or scavenged for nucleotide synthesis.

Results from a 10ppm Maternal Folic Acid Diet

As previously described, there were considerably more metabolite differences between the 10ppm FA control and VPA-exposed mouse embryos than between any other pairwise comparison. Clustering on the 10ppm FA mouse embryo samples and the metabolite abundances for these embryos highlighted these differences (Fig 4). Compounds across most classes, including amino acid and nucleotide metabolism, were found to be decreased in abundance, while compounds in the lipid metabolism class were found at high abundance in the 10ppm VPA-exposed embryo group as compared to the 10ppm FA control group.

VPA has been implicated in altering the metabolism of the neurotransmitter GABA and related metabolites, as well as causing increased oxidative stress and TCA cycle inhibition (Johannessen, 2000; Johannessen and Johannessen, 2003). In GABA metabolism, VPA may alter the synthesis, degradation, and transport of GABA, aspartate, and glutamate as one potential mechanism behind its anti-epileptic action. Therefore, a possible metabolic point of intersection for folic acid and VPA is at glutamine and aspartate, since these amino acids are required for purine and pyrimidine biosynthesis, a process that uses one-carbon groups supplied by tetrahydrofolate. Aspartic acid (Fig 5A), glutamine (Fig 5B), and the related amino acids glutamate, asparagine, alanine, arginine, proline, and histidine (Fig S2A-S2F) were all found to be decreased in abundance in the 10ppm FA VPA-exposed embryo group relative to the 10ppm FA control group. Carbamoyl aspartate, a building block in pyrimidine metabolism that is synthesized from both aspartate and glutamine, was also decreased in abundance in the 10ppm FA VPA-exposed mouse embryos (Fig 5C). TCA cycle components malate (Fig S2G), which can be converted into aspartate, and alpha-ketoglutarate (Fig S2H), which can be converted into glutamate, were also decreased in abundance. Succinate, a product of GABA degradation, was also low in abundance in the VPA-exposed 10ppm FA mouse embryos, compared to control (Fig S2I). However, based on the loading ratio threshold of $-2.0 < PC1/PC2 < 2.0$, aspartate and alpha-ketoglutarate were considered to be somite-linked, which complicated the interpretation of the abundance differences for these molecules.

All diphosphate and triphosphate purine and pyrimidine derivatives were either not detected with confidence in the MS analysis, or were judged to be somite-linked in their abundance. However, UMP (Fig 5D), CMP (Fig 5E), AMP (Fig 5G), and GMP (Fig 5H) were found to be somite-independent based on the negative mode PC1/PC2 ratio, and levels of all were observed to decrease in 10ppm FA VPA-exposed embryos. The only two identified compounds that were found to be significantly different between the 2ppm FA control and VPA-exposed mouse embryos were the nucleobases adenine and thymine. Thymine (Fig 5F) and adenine (Fig 5I) were also decreased in a statistically significant manner in the 10ppm FA VPA-exposed embryos, compared to the 10ppm FA control group.

While the depletion of glutamate, aspartate, and other metabolites related to purine and pyrimidine synthesis may be enough to explain the development of NTDs, the balance of metabolites in 10ppm FA VPA-exposed mouse embryos was perturbed beyond just this group of compounds, as indicated by the clustering analysis depicted in Figure 4. The cluster of compounds marked as being related to lipid metabolism eluted early in aqueous normal phase chromatography, which complicated the confident identification of these molecules.

Regardless of their exact identity, many of these early peaks displayed an abundance pattern similar to that of palmitic acid (Fig 6A), where these hydrophobic molecules were found to be statistically significant based on the folic acid-treatment interaction and were increased in abundance in the 10ppm FA VPA-exposed embryo group, relative to the 10ppm FA control embryos. However, the majority of these molecules had a strong somite-linked component and all confident matches had a PC1/PC2 ratio with an absolute value of less than 2.0.

Weight gain and hepatotoxicity are known side effects of VPA therapy, with disruption of lipid metabolism and mitochondrial beta-oxidation as the likely underlying mechanisms - possibly because VPA is itself at least partially metabolized via beta-oxidation (Bjorge and Baillie, 1991; Silva et al., 2008). To our knowledge, a perturbation in mitochondrial lipid metabolism had not previously been implicated as a potential mechanism by which VPA causes birth defects. Nonetheless, we observed carnitine (Fig 6B), its precursor deoxycarnitine (Fig 6C), and several acyl-carnitines and related metabolites (Table 2) all to be decreased in abundance in the 10ppm FA VPA-exposed embryo group, compared to the 10ppm FA control group. Together with the elevated fatty acid levels, these observations point to perturbed fatty acid beta-oxidation in the 10ppm FA VPA-exposed embryos. Previous research has shown that beta-oxidation of lipids plays a vital role in proper oocyte and early embryo development (Dunning et al., 2010). Notably, a decrease in fatty acid breakdown by beta-oxidation would mean the loss of an important source of ATP and acetyl-CoA for the developing organism, which may also contribute to the relatively low observed levels of TCA cycle intermediates, nucleotides, and amino acids, many of which can be converted to TCA cycle intermediates and salvaged for energy in the 10ppm FA VPA-exposed embryos. While ATP itself was not found to be statistically significantly altered in the 10ppm FA control vs. 10ppm FA VPA-exposed groups, ATP levels were found to be strongly somite-linked. Therefore, no confident conclusions can be drawn on the direct impact of VPA and FA supplementation on ATP levels in the mouse embryos analyzed.

While carnitines can be obtained from dietary sources, they can also be synthesized *de novo* from protein-incorporated trimethyllysine. Because lysine methylation requires methyl groups generated by the one-carbon cycle, carnitine metabolism represents another potential intersection of VPA and folic acid metabolism. Deoxycarnitine, also known as butyrobetaine, is a key precursor of carnitine and alpha-ketoglutarate is required by the enzyme gamma-butyrobetaine dioxygenase for the final step in converting deoxycarnitine to carnitine (Vaz and Wanders, 2002). It is possible that decreased alpha-ketoglutarate limited activity of this biosynthesis pathway, contributing to decreased carnitine abundance. However, deoxycarnitine was also found to be at relatively low abundance in the 10ppm FA VPA-exposed group, compared to the 10ppm FA control (Fig 6C). Additionally, free lysine was detected and also found to be significantly decreased in the 10ppm FA VPA-exposed embryos (Table 2), raising the possibility that lysine incorporation into protein, required for carnitine biosynthesis, may be restrictive. While free trimethyllysine was not detected, the methylation capacity of the embryos could be inferred indirectly based on the relative abundances of S-adenosylmethionine (SAM) and S-adenosylhomocysteine (SAH). SAM and SAH were both decreased in the 10ppm FA VPA-treatment group (Table 2). The SAM/SAH ratio was significant based on the folate parameter only and post-hoc analysis revealed a difference between 2ppm FA and 10ppm FA VPA-exposed groups only (data not

shown). Therefore, while VPA treatment decreased both SAM and SAH in the high folic acid group, the SAM/SAH ratio was not found to be different between the control and the VPA-exposed groups. Homocysteine was not detected with high abundance, but methionine, the immediate product of homocysteine remethylation for continued SAM biosynthesis, was decreased in abundance in the 10ppm FA VPA-exposed group (Table 2). Based on these results, carnitine, and some of its acyl-derivatives, may be found at relatively low abundances in the 10ppm FA VPA-exposed mouse embryos due to attenuated carnitine biosynthesis, potentially arising from limited lysine and SAM availability.

The decreased abundance of SAM and methionine in the 10ppm FA VPA-exposed mouse embryos points to a perturbation in the generation of one-carbon units within the folate cycle. While we did not detect tetrahydrofolate or any of its modified forms in our assays, common one-carbon group and related donors were detected. Notably, serine, glycine, threonine, betaine, and sarcosine (Table 2) were found to be decreased in the 10ppm FA VPA-exposed group when compared to the 10ppm FA control. It should be noted that glycine was strongly somite-linked and, strictly speaking, serine and threonine were borderline somite-linked. Interestingly, choline was detected, but not found to be significantly altered based on Two-Way ANOVA and post hoc testing, suggesting that it was not depleted in order to maintain the betaine and sarcosine levels, although a non-significant p-value should not be taken as evidence of no difference in the abundance of choline between groups. In addition, a number of phosphatidylcholines were detected and not found to be altered in any comparison (data not shown), although lysophosphatidylcholine (LysoPC) 18:0, was elevated in the 10ppm FA VPA group compared to the 10ppm FA control group (Table 2). A lysophosphoethanolamine (LysoPE) 18:0, was also found to be elevated in the 10ppm FA VPA-exposed embryo group compared to the 10ppm FA controls, however this compound was found to be somite-linked with a negative mode PC1/PC2 ratio of 0.84 (data not shown). Together, these data indicate that an interaction between folic acid and VPA treatment can have a profound effect on the one-carbon cycle, leading to a likely decrease of methylation capacity in the 10ppm FA VPA-treatment group, although developmental stage may underlie this finding.

Discussion

There have been conflicting literature reports regarding whether or not folic acid can effectively prevent VPA-associated teratogenesis. Wegner and Nau (1992) suggested that teratogenic doses of VPA alter folate metabolism in the embryo via increasing the level of tetrahydrofolate and decreasing levels of 5-formyl- and 10-formyl-tetrahydrofolates. These changes could be induced by VPA mediated inhibition of transfer of the formyl group via glutamate formyltransferase. A closely related structural analog of VPA (2-en-VPA), which exhibits antiepileptic activity but not teratogenicity, did not adversely impact embryonic folate metabolism (Wegner and Nau, 1992). However, when 5-formyltetrahydrofolate, tetrahydrofolate, 5-methyltetrahydrofolate and folic acid were tested to protect against VPA-induced neural tube defects in mouse and rat embryo culture, none of the folate derivatives were able to decrease the incidence of VPA-induced defects (Hansen, 1993). It has been shown in rats that VPA provoked hepatic DNA hypomethylation, and 5-formyltetrahydrofolate prevented VPA-induced alterations in methionine synthesis and

corrected fetal DNA hypomethylation, suggesting that VPA altered methionine synthase activity (Alonso-Aperte, 1999). Under such conditions, selected genes become more transcriptionally active, which can disrupt the normal developmental program and result in birth defects.

In our study, we investigated the broad consequences of maternal folic acid and VPA treatment on metabolism in day E9.5 mouse embryos. While few differences were observed in embryos from dams maintained on a diet containing 2ppm FA who were VPA-treated and from non-VPA-treated dams, a multitude of metabolic perturbations were detected in 10ppm FA VPA-exposed mouse embryos compared to 2ppm FA VPA-exposed and 10ppm FA control embryos. Therefore, not only did higher folic acid supplementation fail to prevent NTDs in the SWV mouse model, but the 10ppm folic acid diet resulted in a far more profoundly perturbed metabolic outcome than for those embryos exposed *in utero* to VPA in the setting of relatively low folate.

One potential explanation for the relatively few differences detected between 2ppm FA control and VPA-exposed embryos is that the half-life of VPA in mice is only 0.8 hours and the half-life of 2-en-VPA is approximately 1.2 hours (Nau and Zierer, 1982; Nau, 1985). Most metabolic perturbations that contributed to the development of NTDs may have been caused by an acute effect of VPA that disappeared during the 24 hours between treatment and collection due to the brief half-life of the drug and its metabolites. Nonetheless, we were able to detect decreases in the abundance of adenine and thymine in the 2ppm FA VPA-treated group, as compared to the 2ppm FA control group. Therefore, purine and pyrimidine metabolism perturbation may play an important role in VPA-induced teratogenesis. Disruption of nucleotide metabolism would predictably inhibit cell proliferation because nucleotides are required for DNA and RNA synthesis, a process vital for dividing cells. A blockage or slowing of cell proliferation rate may then prevent proper neural tube closure and result in NTDs. A potential additional reason for why few differences between these two groups were detected is that embryo litters from only two dams per group were analyzed in this study. This limited number of pregnancies may have led to either insufficient power because too few embryos were included, or too much variation due to inter-litter differences.

The sheer number of differences between the 10ppm FA control and VPA-exposed mouse embryos make pinpointing the root cause of NTDs in VPA-exposed embryos a challenge. Low levels of aspartate have been shown to retard cell growth, given aspartate's pivotal role in the nucleotide biosynthesis needed for cell proliferation (Birsoy et al., 2015). Glutamine can be used to fuel anabolic reactions, but also can act as a source of energy via conversion to alpha-ketoglutarate and entry into the TCA cycle (Son et al., 2013). Threonine has been shown to be vital for mESC growth in culture because of its contribution to one-carbon units for histone methylation (Shyh-Chang et al., 2013). The list of potential causes of NTDs in the 10ppm FA VPA-exposed groups is far too extensive to be individually discussed, as a large number of key metabolites in central metabolism were found to be low in abundance in these VPA-exposed embryos. Although some of the differences can be attributed to a generalized developmental delay, principal component regression analysis was applied to build the case that many of the metabolite abundance alterations were the result of the dietary intervention and drug administration rather than somite stage. While a somite-

controlled analysis would have been possible in theory, it was not conducted because VPA has previously been associated with a perturbation of somite development (Bruckner et al., 1983; Barnes et al., 1996). Therefore, a developmental delay may be an important mechanism by which VPA causes NTDs and, because no systematic relationship was observed between somite count and all metabolites, the analysis was conducted in such a way as to include as many samples as possible to increase statistical power. There is a precedent for metabolite levels changing as mESCs differentiate in culture (Wang et al., 2009), but the application of principal component regression here was not meant to prove with confidence that certain metabolites are either linked or unrelated to developmental stage. Rather, a somite-linked designation is meant to indicate that the differences in the abundance of such a compound between groups could not be attributed with confidence to experimental intervention alone, and the interpretation was confounded by an embryonic age-related component.

One of the most drastic somite-linked differences was the elevated level of fatty acids observed in embryos from 10ppm FA VPA-treated dams. A possible explanation for this finding is that these high levels of lipids are secondary to VPA treatment and arise as a consequence of developmental delay. However, an alternative hypothesis is that a diminished ability of mouse embryos to consume these fatty acids as a bioenergetic fuel leads to a growth retardation and forces these embryos to resort to scavenging amino acids for energy, thus leading to reduced biosynthesis of purines and pyrimidines. Mitochondrial beta-oxidation has been shown to be important for mouse oocyte and early mouse embryo growth and, in general, mitochondrial beta-oxidation can provide a large quantity of acetyl-CoA and ATP to fuel growth and development. There are a number of proposed mechanisms by which VPA has been suggested to disrupt mitochondrial beta-oxidation, including CoA sequestration, carnitine depletion (inasmuch as carnitine can be conjugated to VPA for transport into the mitochondria like any other fatty acids) (Lheureux et al., 2005), and the formation of metabolites, such as valproyl-CoA, that inhibit enzymes in the fatty acid beta-oxidation pathway (Ponchaut et al., 1992; Silva et al., 2008; Aires et al., 2010; Schumacher and Guo, 2015). While the methodologies applied in this study did not detect CoA, CoA conjugates, or long-chain carnitine conjugates, it is notable that levels of free carnitine and short-chain acyl-carnitines were found to be significantly depleted. These data indicate that VPA may have disturbed carnitine biosynthesis, but it cannot be ruled out that mitochondrial beta-oxidation was additionally attenuated in the 10ppm FA VPA-exposed embryos due to CoA or carnitine sequestration in long-chain fatty acid conjugates. Interestingly, carnitine has been co-administered with valproic acid to treat hyperammonemia linked to increased metabolism of glutamine (Mock and Schwetschenau, 2012), and a future avenue of study would be to investigate the role of mitochondrial beta-oxidation in neural tube closure and NTDs, as well as if carnitine supplementation can effectively attenuate the risk of VPA-induced NTDs. As folic acid only appears to exacerbate, rather than contribute protection to the embryo from VPA-induced NTDs, finding a safe and effective alternative would be a tremendous clinical intervention for the tens of thousands of pregnancies complicated by *in utero* VPA exposure annually.

Related to our finding of perturbed fatty acid metabolism in 10ppm FA VPA-exposed embryos, previous work has shown that a diet of 20 mg/kg of folic acid (comparable to 20

ppm) administered on a genetic background of an MTHFR deficiency (the enzyme which catalyzes the conversion of 5,10-methylenetetrahydrofolate to 5-methyltetrahydrofolate), results in disrupted lipid metabolism in adult mice and induces fatty livers (Christensen et al., 2015). The authors of this work implicated altered methylation of genes that were involved in lipid metabolism as the cause of the disorder, and suggested that unmetabolized folic acid may inhibit MTHFR. With this in mind, perhaps the interaction of folic acid and VPA in the present experiment was not due to a direct action on the metabolite levels, but rather an indirect action mediated at the level of epigenetic regulation. Indeed, VPA is an inhibitor of some HDAC enzyme family members, regulators of protein acetylation levels (Gottlicher et al., 2001; Phiel et al., 2001). HDACs induce transcriptional repression principally by deacetylation of lysine residues on histone tails, which leads to chromatin condensation. Several studies have shown that drugs modulating the acetylation status of histones, including HDAC inhibitors, can inhibit cell growth and induce terminal differentiation, adversely altering the normal pattern of embryonic development (Menegola et al., 2006; Di Renzo et al., 2007). Menegola and colleagues showed a direct correlation between somite hyperacetylation and axial abnormalities, further supporting a role of HDAC inhibition as a mechanism by which the VPA may exerts its teratogenic effects (Menegola et al., 2005).

Folic acid is converted to tetrahydrofolate in the organism, a carrier for one carbon units required for reactions central to epigenetic regulation and cell growth. Methylation patterns in mouse embryos are dynamic (Santos et al., 2002) and a reasonable hypothesis is that higher levels of folic acid and tetrahydrofolate result in an altered methylation profile from that with relatively low folic acid supplementation, changing an organism's response to VPA administration. Although the 2ppm and 10ppm maternal FA diets did not give rise to NTDs on their own and did not result in statistically significant metabolic differences in the control embryos, they did engender a statistically significant change in metabolite levels between the two supplementation levels after VPA treatment. Conceivably, the most drastic changes in metabolites observed in the 10ppm FA VPA-exposed mouse embryos could have been caused by altered methylation of DNA or histones in a manner that left these embryos more susceptible to a single treatment of VPA. In addition, the effect on methylation need not be limited to an action on the mouse embryos alone. A higher level of folic acid supplementation may have altered epigenetic modifications of the mother's DNA, which left the dam more vulnerable to metabolic perturbations by VPA. Since mouse embryos receive all of their nutrients from their mother, disturbance in the dam's metabolism can result in a disruption of the embryo's metabolism.

In summary, we present a broad metabolomic analysis of mouse embryos from VPA-treated dams and assessment of low and high folic acid diet on treatment outcomes. Regardless of folic acid supplementation level, a single VPA dose on day E8.5 of gestation was sufficient to induce NTDs in all resultant mouse embryos. Surprisingly, not only did increased folic acid supplementation not prevent NTDs, but paradoxically, it greatly amplified metabolic profile differences that arise with maternal VPA treatment. One possible explanation for this unexpected finding was that a high folic acid diet perturbs lipid metabolism and, in combination with VPA-mediated carnitine depletion, more profoundly disturbs energy metabolism. One-carbon metabolism, particularly purine and pyrimidine biosynthesis, was

also disrupted, possibly due to the altered cell bioenergetics and depletion of key amino acids that are required for nucleotide biosynthesis. Another possible explanation for the observations seen here is that altered methylation of DNA and proteins left the dam, embryos, or both, susceptible to an acute assault by VPA. While the teratogenic mechanism of action for VPA remains speculative, it is important to realize that multiple mechanisms of VPA teratogenicity may be at play and act in synergy.

Supplementary Material

Refer to Web version on PubMed Central for supplementary material.

Acknowledgments

Literature Cited

Aires CC, Ijlst L, Stet F, Prip-Buus C, de Almeida IT, Duran M, Wanders RJ, Silva MF. Inhibition of hepatic carnitine palmitoyl-transferase I (CPT IA) by valproyl-CoA as a possible mechanism of valproate-induced steatosis. Biochem Pharmacol. 2010; 79(5)

Alonso-Aperte E, Ubeda N, Achón M, Pérez-Miguelsanz J, Varela-Moreiras G. Impaired methionine synthesis and hypomethylation in rats exposed to valproate during gestation. Neurology. 1999; 52(4):750–6. [PubMed: 10078722]

Barnes GL, Mariani BD, Tuan RS. Valproic acid-induced somite teratogenesis in the chick embryo: Relationship with pax-1 gene expression. Teratology. 1996; 54(2):93–102. [PubMed: 8948545]

Birsoy K, Wang T, Chen WW, Freinkman E, Abu-Remaileh M, Sabatini DM. An Essential Role of the Mitochondrial Electron Transport Chain in Cell Proliferation Is to Enable Aspartate Synthesis. Cell. 2015; 162(3):540–551. [PubMed: 26232224]

Bjorge SM, Baillie TA. Studies on the beta-oxidation of valproic acid in rat liver mitochondrial preparations. Drug metabolism and disposition: the biological fate of chemicals. 1991; 19(4):823–829. [PubMed: 1680661]

Bruckner A, Lee YJ, O'Shea KS, Henneberry RC. Teratogenic effects of valproic acid and diphenylhydantoin on mouse embryos in culture. Teratology. 1983; 27(1):29–42. [PubMed: 6405496]

Buourgeois, BFD. Valproic acid: clinical efficacy and use in epilepsy. In: Levy, RH.Mattson, RH.Meldrum, BS., Perucca, E., editors. Antiepileptic Drugs. 5th ed.. Lippincott Williams & Wilkins; Philadelphia, PA: 2002. p. 808-817.

Christensen KE, Mikael LG, Leung KY, Levesque N, Deng L, Wu Q, Malysheva OV, Best A, Caudill MA, Greene ND, Rozen R. High folic acid consumption leads to pseudo-MTHFR deficiency, altered lipid metabolism, and liver injury in mice. Am J Clin Nutr. 2015; 101(3):646–658. [PubMed: 25733650]

Copp AJ, Stanier P, Greene NDE. Neural tube defects: recent advances, unsolved questions, and controversies. The Lancet Neurology. 2013; 12(8):799–810. [PubMed: 23790957]

Dunning KR, Cashman K, Russell DL, Thompson JG, Norman RJ, Robker RL. Beta-oxidation is essential for mouse oocyte developmental competence and early embryo development. Biol Reprod. 2010; 83(6):909–918. [PubMed: 20686180]

Elmazar MM, Thiel R, Nau H. Effect of supplementation with folinic acid, vitamin B6, and vitamin B12 on valproic acid-induced teratogenesis in mice. Fundamental and applied toxicology : official journal of the Society of Toxicology. 1992; 18(3):389–394. [PubMed: 1597263]

Fathe K, Palacios A, Finnell RH. Brief report novel mechanism for valproate-induced teratogenicity. Birth Defects Research Part A: Clinical and Molecular Teratology. 2014; 100(8):592–597. [PubMed: 25066307]

Göttlicher M, Minucci S, Zhu P, Krämer OH, Schimpf A, Giavara S, Sleeman JP, Lo Coco F, Nervi C, Pelicci PG, Heinzel T. Valproic acid defines a novel class of HDAC inhibitors inducing differentiation of transformed cells. The EMBO journal. 2001; 20(24):6969–6978. [PubMed: 11742974]

Greene ND, Copp AJ. Neural tube defects. Annu Rev Neurosci. 2014; 37:221–242. [PubMed: 25032496]

Hansen DK. In vitro effects of folate derivatives on valproate-induced neural tube defects in mouse and rat embryos. Toxic in Vitro. 1993; 7(6):735–742.

Hansen DK, Grafton TF, Dial SL, Gehring TA, Siitonen PH. Effect of supplemental folic acid on valproic acid-induced embryotoxicity and tissue zinc levels in vivo. Teratology. 1995; 52(5):277–285. [PubMed: 8838251]

Hansler A, Chen Q, Gray JD, Ross EM, Finnell RH, Gross SS. Untargeted metabolite profiling of murine embryos to reveal metabolic perturbations associated with neural tube closure defects. Birth Defects Research Part A: Clinical and Molecular Teratology. 2014; 100(8):623–632. [PubMed: 25115437]

Jentink J, Bakker MK, Nijenhuis CM, Wilffert B, de Jong-van den Berg LT. Does folic acid use decrease the risk for spina bifida after in utero exposure to valproic acid? Pharmacoepidemiol Drug Saf. 2010a; 19(8):803–807. [PubMed: 20680999]

Jentink J, Loane MA, Dolk H, Barisic I, Garne E, Morris JK, de den Berg LTW, Group E. Valproic Acid Monotherapy in Pregnancy and Major Congenital Malformations. The New England Journal of Medicine. 2010b; 362(23):2185–2193. [PubMed: 20558369]

Johannessen CU. Mechanisms of action of valproate: a commentatory. Neurochemistry international. 2000; 37(2-3):103–110. [PubMed: 10812195]

Johannessen CU, Johannessen SI. Valproate: past, present, and future. CNS drug reviews. 2003; 9(2): 199–216. [PubMed: 12847559]

Lheureux PE, Penaloza A, Zahir S, Gris M. Science review: carnitine in the treatment of valproic acid-induced toxicity – what is the evidence? Crit Care. 2005; 9(5):431–40. [PubMed: 16277730]

Lloyd K. A scientific review: mechanisms of valproate-mediated teratogenesis. Bioscience Horizons. 2013; 6(0)

Marson, AG., Sills, GJ. Chapter 51: Valproate. In: Shorvon, S.Perucca, E., Engel, J., editors. The Treatment of Epilepsy. 4th ed. John Wiley & Sons, Ltd; 2015. p. 652-666.

Mock CM, Schwetschenau KH. Levocarnitine for valproic-acid-induced hyperammonemic encephalopathy. Am J Health Syst Pharm. 2012; 69(1):35–39. [PubMed: 22180549]

Nau H. Teratogenic valproic acid concentrations: infusion by implanted minipumps vs conventional injection regimen in the mouse. Toxicol Appl Pharmacol. 1985; 80(2):243–50. [PubMed: 3927520]

Nau H, Zierer R. Pharmacokinetics of valproic acid and metabolites in mouse plasma and brain following constant-rate application of the drug and its unsaturated metabolite with an osmotic delivery system. Biopharm Drug Dispos. 1982; 3(4):317–28. [PubMed: 6819013]

Ornoy A. Valproic acid in pregnancy: how much are we endangering the embryo and fetus? Reprod Toxicol. 2009; 28(1):1–10. [PubMed: 19490988]

Ponchaut S, van Hoof F, Veitch K. In vitro effects of valproate and valproate metabolites on mitochondrial oxidations. Relevance of CoA sequestration to the observed inhibitions. Biochem Pharmacol. 1992; 43(11)

Price KE, Pearce RE, Garg UC, Heese BA, Smith LD, Sullivan JE, Kennedy MJ, Bale JF Jr. Ward RM, Chang TK, Abbott FS, Leeder JS. Effects of valproic acid on organic acid metabolism in children: a metabolic profiling study. Clin Pharmacol Ther. 2011; 89(6):867–874. [PubMed: 21544075]

Reeves PG. Components of the AIN-93 diets as improvements in the AIN-76A diet. The Journal of nutrition. 1997; 127(5 Suppl)

Sadler TW. Embryology of neural tube development. Am J Med Genet C Semin Med Genet. 2005; 135C(1):2–8. [PubMed: 15806586]

Santos F, Hendrich B, Reik W, Dean W. Dynamic reprogramming of DNA methylation in the early mouse embryo. Developmental biology. 2002; 241(1):172–182. [PubMed: 11784103]

Schumacher JD, Guo GL. Mechanistic review of drug-induced steatohepatitis. Toxicol Appl Pharmacol. 2015; 289(1)

Shyh-Chang N, Locasale JW, Lyssiotis CA, Zheng Y, Teo RY, Ratanasirintrawoot S, Zhang J, Onder T, Unternaehrer JJ, Zhu H, Asara JM, Daley GQ, Cantley LC. Influence of Threonine Metabolism on S-Adenosylmethionine and Histone Methylation. Science. 2013; 339(6116):222–226. [PubMed: 23118012]

Silberstein, SD. Valproic acid: clinical efficacy and use in other neurological disorders. In: Levy, RH.Mattson, RH.Meldrum, BS., Perucca, E., editors. Antiepileptic Drugs. Lippincott Williams & Wilkins; Philadelphia, PA: 2002. p. 818-827.

Silva MF, Aires CC, Luis PB, Ruiter JP, L IJ, Duran M, Wanders RJ, Tavares de Almeida I. Valproic acid metabolism and its effects on mitochondrial fatty acid oxidation: a review. J Inherit Metab Dis. 2008; 31(2):205–216. [PubMed: 18392741]

Son J, Lyssiotis CA, Ying H, Wang X, Hua S, Ligorio M, Perera RM, Ferrone CR, Mullarky E, Shyh-Chang N, Kang Y, Fleming JB, Bardeesy N, Asara JM, Haigis MC, DePinho RA, Cantley LC, Kimmelman AC. Glutamine supports pancreatic cancer growth through a KRAS-regulated metabolic pathway. Nature. 2013; 496(7443):101–105. [PubMed: 23535601]

Swann, AC. Valproic acid: clinical efficacy and use in psychiatric disorders. In: Levy, RH.Mattson, RH.Meldrum, BS., Perucca, E., editors. Antiepileptic Drugs. Lippincott Williams & Wilkins; Philadelphia, PA: 2002. p. 827-836.

Tung EW, Winn LM. Valproic acid increases formation of reactive oxygen species and induces apoptosis in postimplantation embryos: a role for oxidative stress in valproic acid-induced neural tube defects. Mol Pharmacol. 2011; 80(6):979–987. [PubMed: 21868484]

Vaz FM, Wanders RJA. Carnitine biosynthesis in mammals. Biochemical Journal. 2002; 361(3):417–429. [PubMed: 11802770]

Wallingford JB, Niswander LA, Shaw GM, Finnell RH. The Continuing Challenge of Understanding, Preventing, and Treating Neural Tube Defects. Science. 2013; 339:1222002. [PubMed: 23449594]

Wang J, Alexander P, Wu L, Hammer R, Cleaver O, McKnight SL. Dependence of mouse embryonic stem cells on threonine catabolism. Science. 2009; 325(5939):435–439. [PubMed: 19589965]

Wegner C, Nau H. Alteration of embryonic folate metabolism by valproic acid during organogenesis: implications for mechanism of teratogenesis. Neurology. 1992; 42:17–24.

Wilde JJ, Petersen JR, Niswander L. Genetic, epigenetic, and environmental contributions to neural tube closure. Annu Rev Genet. 2014; 48:583–611. [PubMed: 25292356]
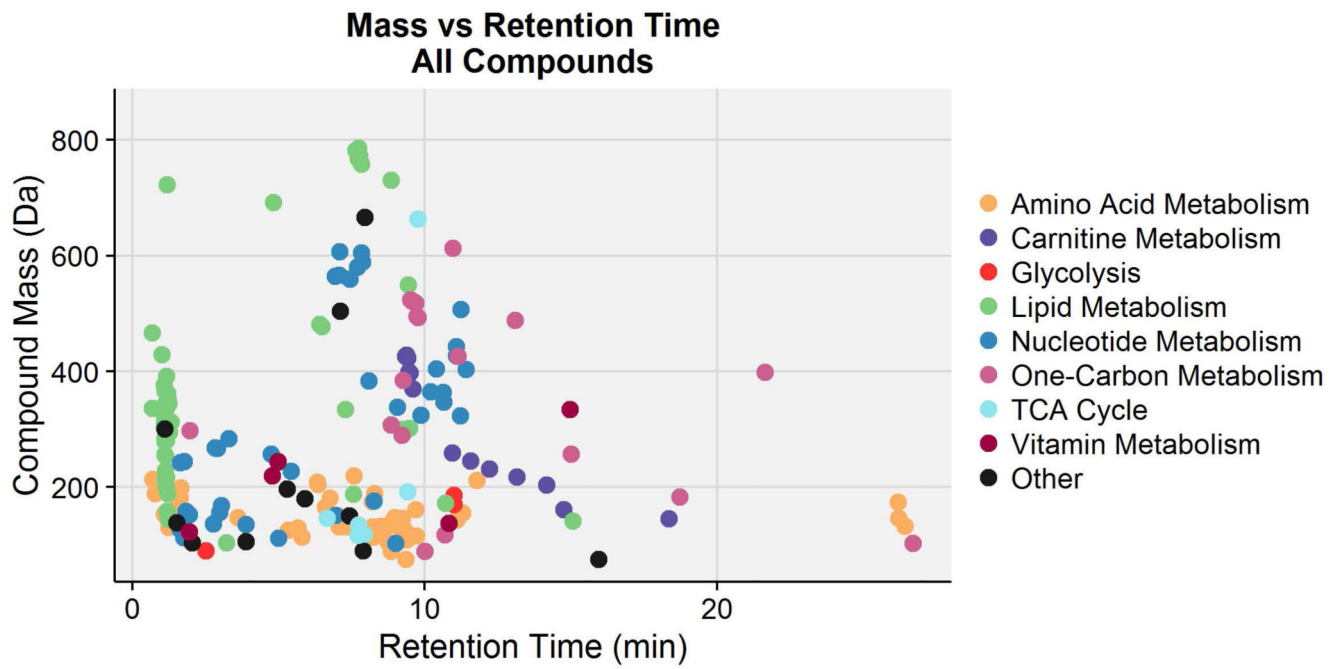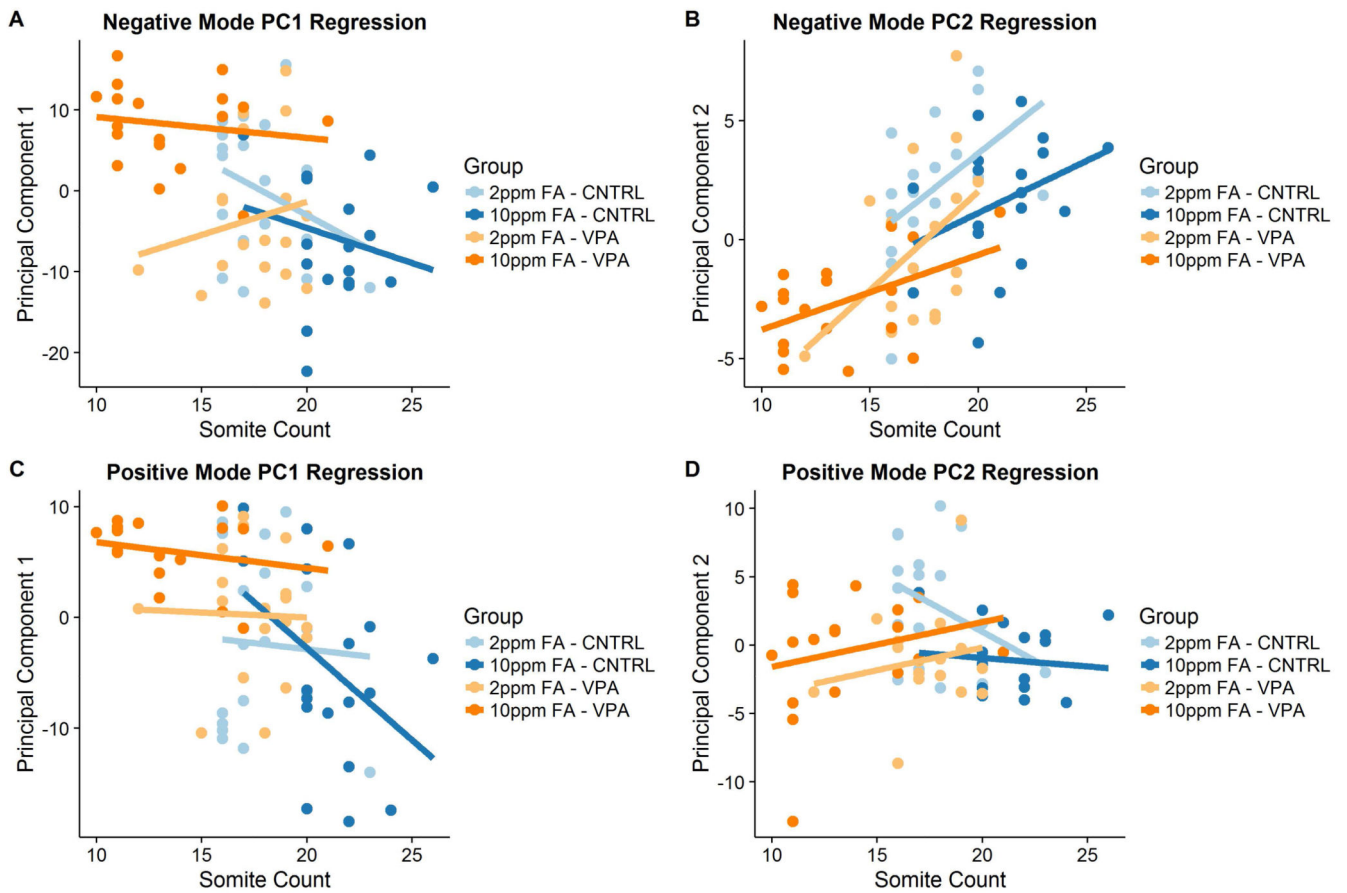
Figure 1.
Compound mass vs. retention time plot for 200 compounds with unique masses and retention times, identified by positive- and negative-ion mode LC/MS. These compounds are annotated by color based on their major metabolic classifications.
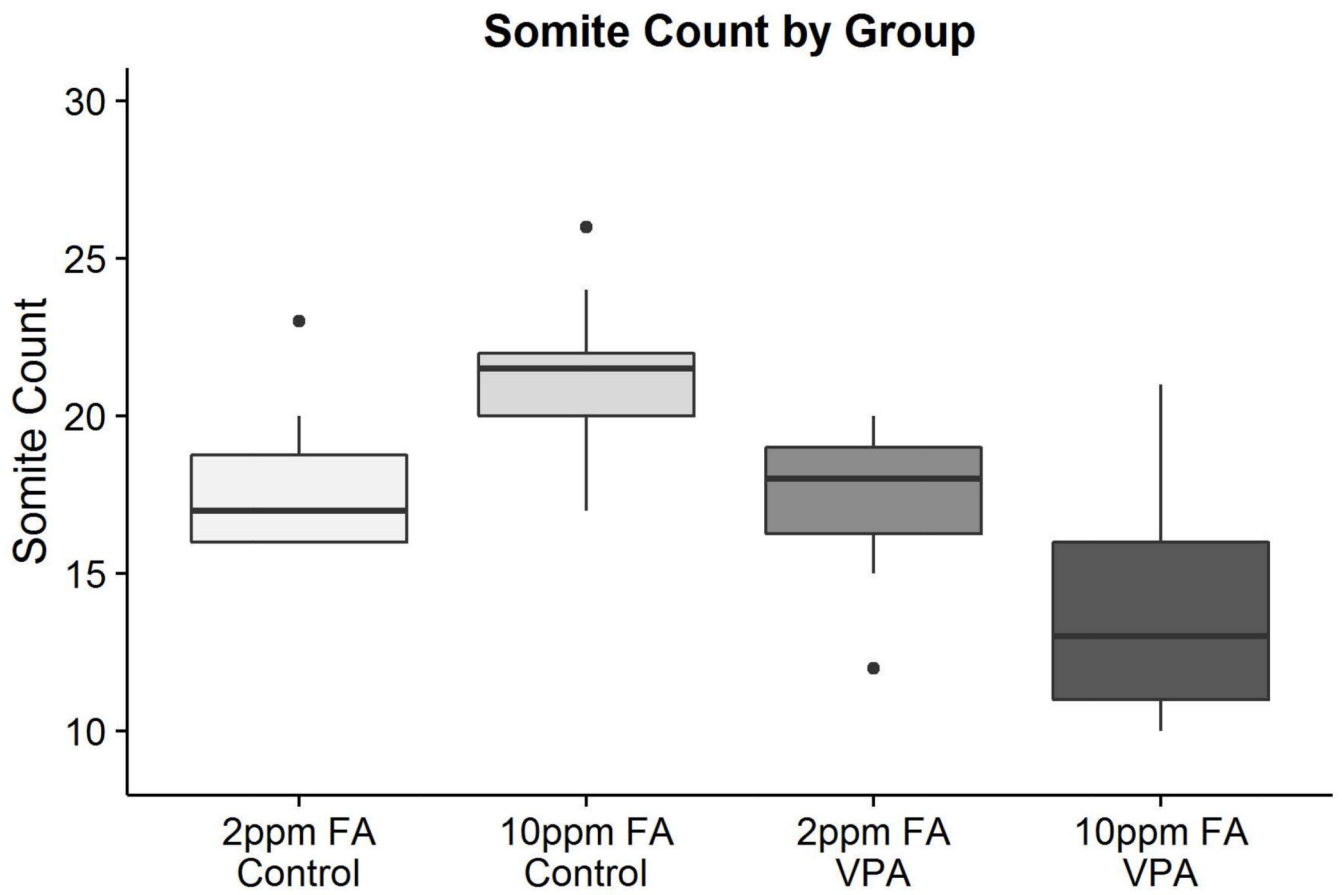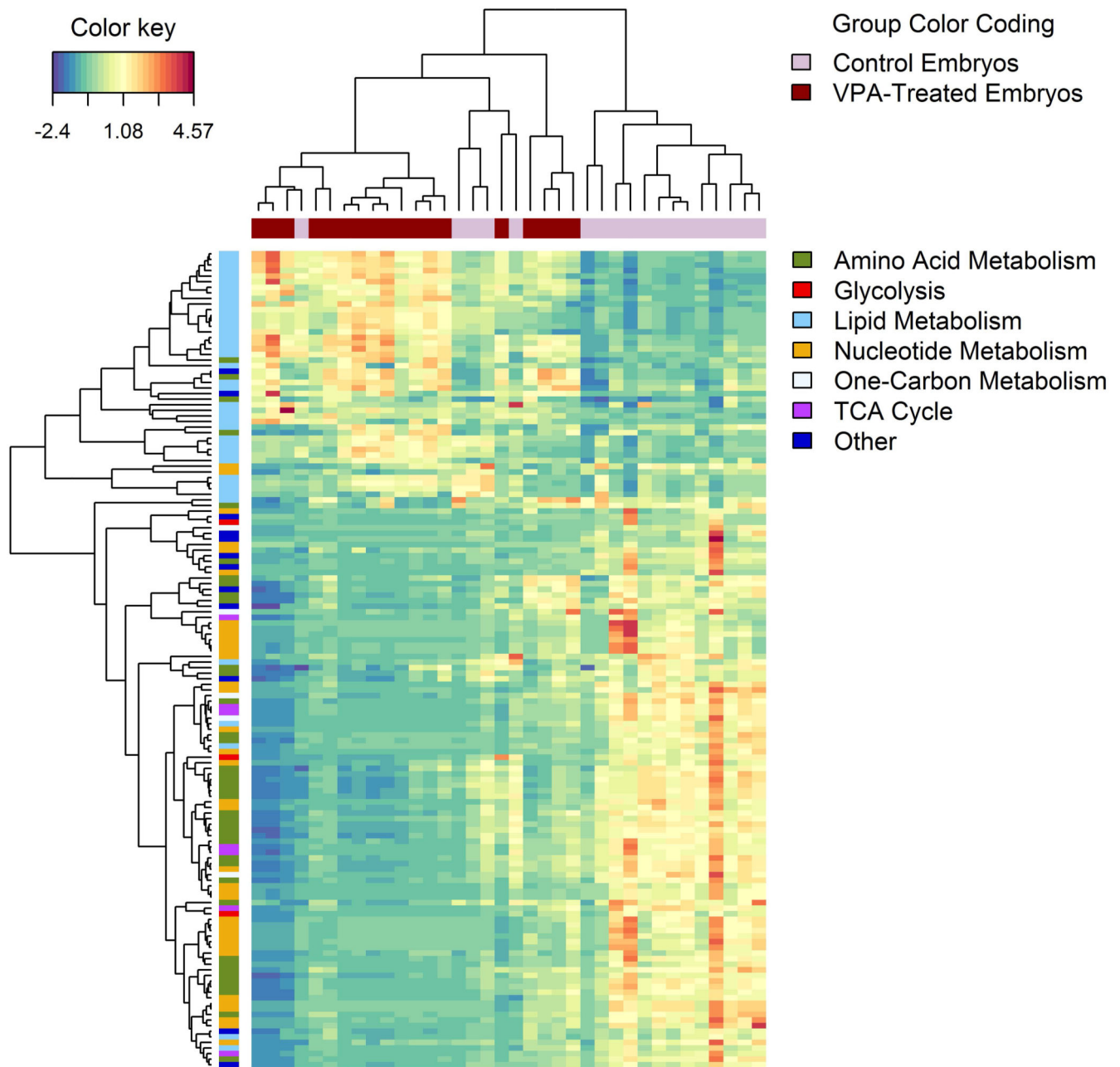
Figure 2.
Boxplots depicting the somite count of murine embryos in each of the four treatment groups included in the LC/MS metabolomics analysis. All pairwise comparisons are statistically significant with the exception of 2ppm FA Control and 2ppm FA VPA (n = 18 for each group). Exact differences in somite count and p-values can be found in Supplementary Table 1.
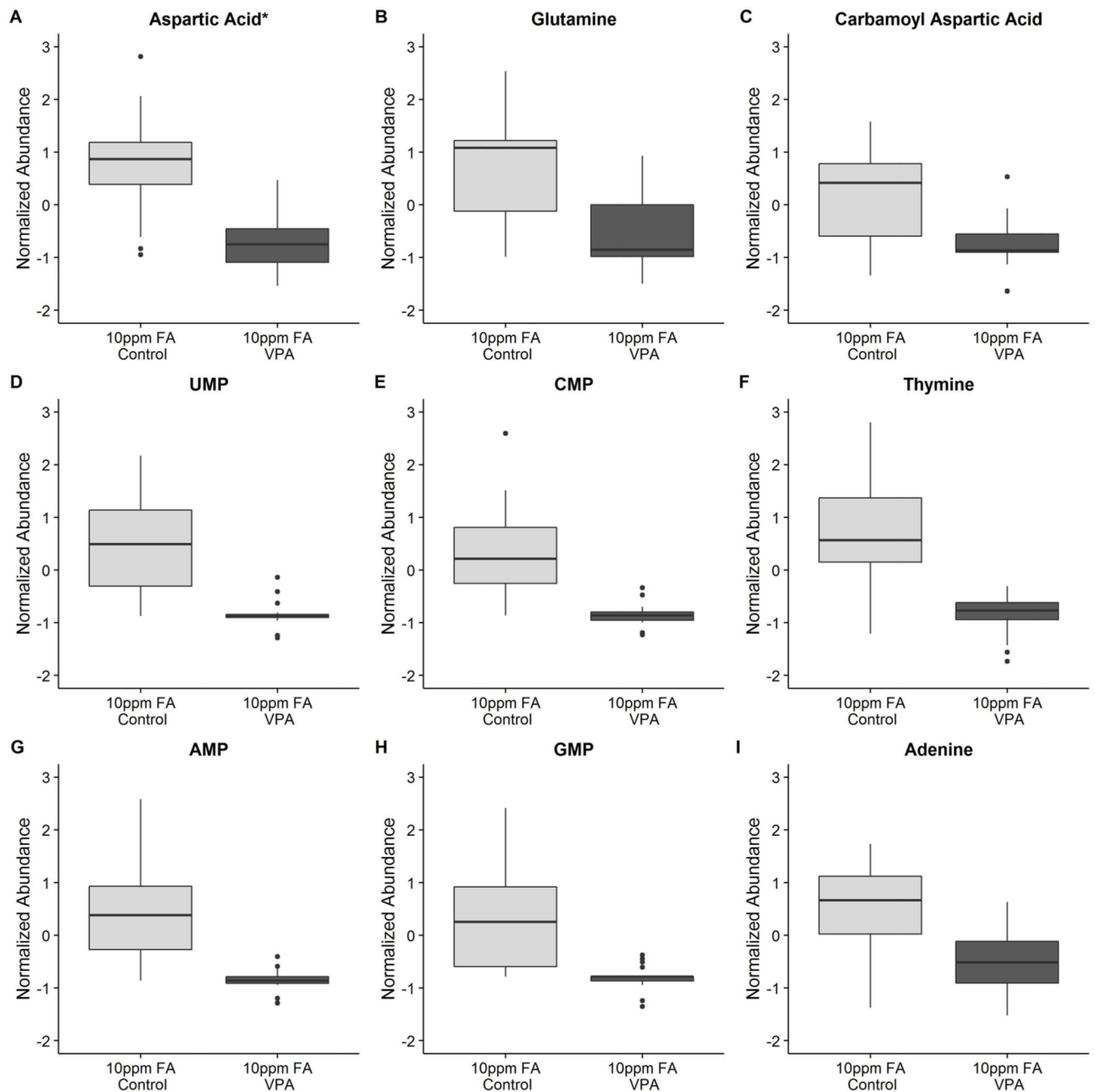
Figure 3.
Principal component (PC1 and PC2) regression onto somite counts for control and VPA-exposed mouse embryos from dams receiving a diet containing either 2ppm or 10ppm FA. **(A)** PC1 based on negative mode data (59.9% of all variance explained), no significant regression or meaningful R^2 for any group. **(B)** PC2 based on negative mode data (7.6% of all variance explained), 2ppm FA – CNTRL $R^2 = 0.23$, no significant regression for the 10ppm FA – CNTRL group, 2ppm FA – VPA $R^2 = 0.24$, 10ppm FA – VPA $R^2 = 0.22$. **(C)** PC1 based on positive mode data (49.5% of all variance explained), no significant regression or meaningful R^2 for any group. **(D)** PC2 based on positive mode data (13.4% of all variance explained), no significant regression or meaningful R^2 for any group. (n = 18 embryos for each group.)

Figure 4.
Untargeted hierarchical clustering plot demonstrating alterations in the relative abundances of compounds in embryos from VPA-treated vs. control dams receiving a diet containing10ppm FA. Depicted results were represented as a heat map based on compounds identified with negative-ion mode LC/MS analysis. In this data representation, metabolites are clustered in the rows and 10ppm FA control and VPA-exposed embryos are clustered in the columns. Pearson correlation and complete linkage was used to cluster both columns and rows. Compounds in the rows are also marked by major compound classifications. (n = 18 embryos for each group.)
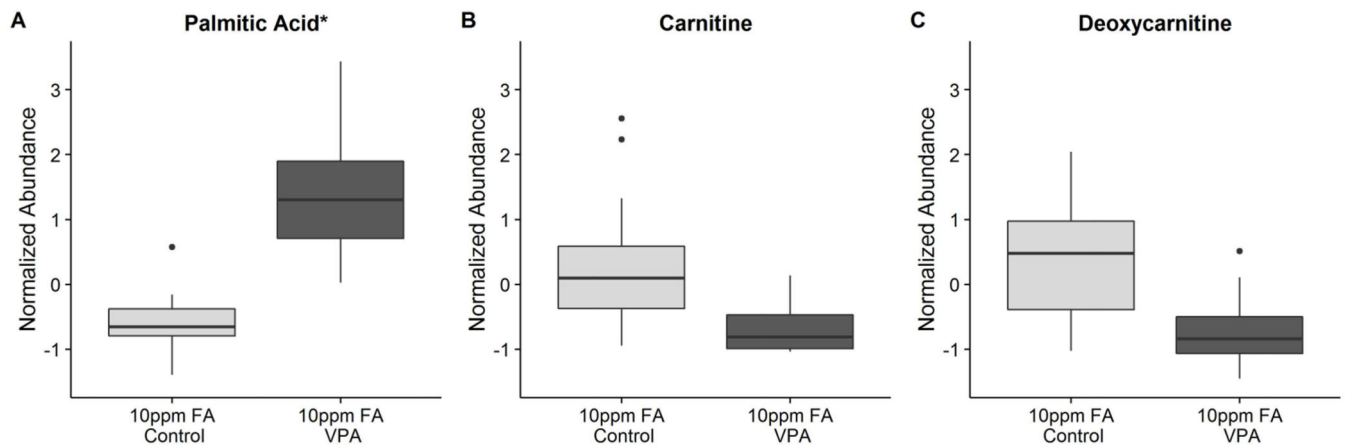
Figure 5.
Boxplots describing the relative abundance changes in compounds related to purine and pyrimidine metabolism in embryos from VPA-treated vs. control dams supplemented with 10ppm FA. **(A)** Aspartic acid: p-val (Tukey HSD) = 7.46×10^{-5}, Neg mode PC1/PC2 = -1.85 (somite-linked). **(B)** Glutamine: p-val (Tukey HSD) = 0.0016, Neg mode PC1/PC2 = -27.73. **(C)** Carbamoyl aspartic acid: p-val (Tukey HSD) = 0.0083, Neg mode PC1/PC2 = -2.88. **(D)** UMP: p-val (Tukey HSD) = 5.01×10^{-4}, Neg mode PC1/PC2 = -2.60. **(E)** CMP: p-val (Tukey HSD) = 0.0014, Neg mode PC1/PC2 = -3.45. **(F)** Thymine: p-val (t-test) = 6.87×10^{-4}, Pos mode data. **(G)** AMP: p-val (Tukey HSD) = 0.0014, Neg mode PC1/PC2 =

−3.72. **(H)** GMP: p-val (Tukey HSD) = 0.0024, Neg mode PC1/PC2 = −3.87. **(I)** Adenine: p-val (t-test) = 0.0013, Pos mode data. *Indicates a somite-linked compound. (n = 18 embryos for each group).

Figure 6.
Boxplots describing the relative abundance changes in compounds related to lipid and carnitine metabolism in embryos from VPA-treated vs. control dams supplemented with 10ppm FA. **(A)** Palmitic acid: p-val (Tukey HSD) = app. 0, Neg mode PC1/PC2 = −1.01 (somite-linked). **(B)** Carnitine: p-val (t-test) = 0.0018, Pos mode data. **(C)** Deoxycarnitine: p-val (t-test) = 0.0013, Pos mode data. *Indicates a somite-linked compound. (n = 18 embryos for each group).

Table 1

Statistically significant metabolites from the comparison of 2ppm FA control vs 2ppm FA VPA-exposed embryo extracts

Compound	Control Mean (scaled units)[*]	VPA Mean (scaled units)[*]	Change from Control to VPA	Difference[**] (scaled units)[*]	P-value (Corrected)
Adenine	0.86	−0.67	Down	1.52 (95% CI = 1.00 to 2.10)	7.91×10^{-5} (t-test)
Thymine	0.67	−0.33	Down	1.01 (95% CI = 0.55 to 1.56)	0.012 (t-test)

n = 18 for each group.

[*] Metabolite measurements are in z-scaled units.

[**] Arithmetic difference between the control mean and the VPA mean for each compound with the 95% CI for the difference included.

Table 2

Statistically significant metabolites linked to carnitine and one-carbon metabolism from the comparison of 10ppm FA control vs 10ppm FA VPA-exposed embryo extracts

Compound	Control Mean (scaled units)[*]	VPA Mean (scaled units)[*]	Change from Control to VPA	Difference[**] (scaled units)[*]	P-value (Corrected)
Acetylcarnitine	0.13	−0.67	Down	0.80 (95% CI = 0.30 to 1.24)	0.0077 (t-test)
Butyrylcarnitine	0.50	−0.75	Down	1.26 (95% CI = 0.47 to 2.05)	0.0011 (Tukey HSD)
Hexanoylcarnitine	0.47	−0.78	Down	1.25 (95% CI = 0.67 to 1.73)	0.0013 (t-test)
Propionylcarnitine	0.28	−0.61	Down	0.89 (95% CI = 0.30 to 1.38)	0.0100 (t-test)
Pentanoylcarnitine	0.48	−0.63	Down	1.12 (95% CI = 0.44 to 1.73)	0.0061 (t-test)
Lysine (PC1/PC2 = −5.19)	0.62	−0.80	Down	1.42 (95% CI = 0.65 to 2.20)	1.32×10^{-4} (Tukey HSD)
SAM	0.74	−0.63	Down	1.37 (95% CI = 0.58 to 2.16)	4.40×10^{-4} (Tukey HSD)
SAH	1.11	−0.54	Down	1.65 (95% CI = 0.91 to 2.38)	2.08×10^{-5} (Tukey HSD)
Methionine	0.47	−0.71	Down	1.18 (95% CI = 0.54 to 1.79)	0.0024 (t-test)
Serine[*] (PC1/PC2 = −1.90)	0.70	−0.83	Down	1.53 (95% CI = 0.78 to 2.28)	2.23×10^{-5} (Tukey HSD)
Glycine[*] (PC1/PC2 = −0.82)	0.63	−0.67	Down	1.31 (95% CI = 0.48 to 2.13)	9.50×10^{-4} (Tukey HSD)
Threonine[*] (PC1/PC2 = −1.85)	0.89	−0.80	Down	1.69 (95% CI = 0.95 to 2.43)	2.66×10^{-6} (Tukey HSD)
Betaine	0.31	−0.82	Down	1.14 (95% CI = 0.62 to 1.58)	0.0013 (t-test)
Sarcosine	0.56	−0.80	Down	1.36 (95% CI = 0.77 to 1.90)	0.0013 (t-test)
LysoPC (18:0)	−0.45	0.46	Up	−0.92 (95% CI = −0.13 to −1.70)	0.024 (Tukey HSD)

n = 18 for each group.

[*] Metabolite measurements are in z-scaled units.

[**] Arithmetic difference between the control mean and the VPA mean for each compound with the 95% CI for the difference included.